Food Chemistry 237 (2017) 390–398

Contents lists available at ScienceDirect

Food Chemistry

journal homepage: www.elsevier.com/locate/foodchem

Antioxidative mechanisms in chlorogenic acid

Jelena Tošović [a,*], Svetlana Marković [a], Jasmina M. Dimitrić Marković [b], Miloš Mojović [b], Dejan Milenković [c]

[a] University of Kragujevac, Faculty of Science, Department of Chemistry, 12 Radoja Domanovića, 34000 Kragujevac, Serbia
[b] Faculty of Physical Chemistry, University of Belgrade, 12-16 Studentski trg, 11000 Belgrade, Serbia
[c] Bioengineering Research and Development Centre, 6 Prvoslava Stojanovića, 34000 Kragujevac, Serbia

ARTICLE INFO

Article history:
Received 13 February 2017
Received in revised form 26 April 2017
Accepted 16 May 2017
Available online 20 May 2017

Chemical compounds studied in this article:
5-*O*-caffeoylquinic acid (PubChem CID: 1794427)

Keywords:
ESR experiment
DFT calculations
Thermodynamic approach
Kinetic approach

ABSTRACT

Although chlorogenic acid (**5CQA**) is an important ingredient of various foods and beverages, mechanisms of its antioxidative action have not been fully clarified. Besides electron spin resonance experiment, this study includes thermodynamic and mechanistic investigations of the hydrogen atom transfer (HAT), radical adduct formation (RAF), sequential proton loss electron transfer (SPLET), and single electron transfer – proton transfer (SET-PT) mechanisms of **5CQA** in benzene, ethanol, and water solutions. The calculations were performed using the M06-2X/6-311++G(d,p) level of theory and CPCM solvation model. It was found that SET-PT is not a plausible antioxidative mechanism of **5CQA**. RAF pathways are faster, but HAT yields thermodynamically more stable radical products, indicating that in acidic and neutral media **5CQA** can take either HAT or RAF pathways. In basic environment (e.g. at physiological pH) SPLET is the likely antioxidative mechanism of **5CQA** with extremely high rate.

1. Introduction

In living organisms, reactive oxygen species are formed in a wide range of reactions. Superoxide radical anion is mainly formed in the electron transport chains during cellular respiration, when an oxygen molecule takes up one electron. At pH = 4.8, $O_2^{\cdot-}$ is in equilibrium with the more potent hydroperoxyl radical:

$$O_2^{\cdot-} + H^+ \leftrightarrows HOO^{\cdot} \quad (1)$$

implying that $O_2^{\cdot-}$ prevails at larger pH values (e.g. under physiological conditions), whereas $HOO^{\cdot}$ prevails in acidic media. In numerous plant and animal tissues $O_2^{\cdot-}$ undergoes enzymatic dismutation:

$$2O_2^{\cdot-} + 2H^+ \rightarrow H_2O_2 + O_2 \quad (2)$$

Hydrogen peroxide can undergo Fenton reaction:

$$Fe^{2+} + H_2O_2 \rightarrow Fe^{3+} + HO^{\cdot} + HO^- \quad (3)$$

and Haber-Weiss reaction:

$$H_2O_2 + O_2^{\cdot-} \xrightarrow{\text{Fe catalyst}} HO^{\cdot} + HO^- + O_2 \quad (4)$$

In both processes a powerful oxidant, the hydroxyl radical, is formed.

Antioxidants are characterized with many beneficial properties related to their ability to inhibit oxidative stress and associated molecular damage. Polyphenols are an important group of antioxidants that realize their antioxidative action via several mechanisms (Fifen, Nsangou, Dhaouadi, Motopon, & Jaidane, 2011; Galano & Alvarez-Idaboy, 2013; Galano et al., 2016; Mazzone, Malaj, Galano, Russo, & Toscano, 2015; Leopoldini, Russo, & Toscano, 2011; Litwinienko & Ingold, 2007). The hydrogen atom transfer [HAT, Eq. (5)], radical adduct formation [RAF, Eq. (6)], sequential proton loss electron transfer [SPLET, Eqs. (7)–(9)], and single electron transfer – proton transfer [SET-PT, Eqs. (10) and (11)] mechanisms in chlorogenic acid (5-*O*-caffeoylquinic acid, **5CQA**) are the subject of the present investigation.

$$\mathbf{5CQA} + R^{\cdot} \rightarrow \mathbf{5CQA}^{\cdot} + RH \quad (5)$$

$$\mathbf{5CQA} + R^{\cdot} \rightarrow (\mathbf{5CQA} - \mathbf{R})^{\cdot} \quad (6)$$

$$\mathbf{5CQA} \leftrightarrows \mathbf{5CQA}^- + H^+ \quad (7)$$

$$\mathbf{5CQA}^- + R^{\cdot} \rightarrow \mathbf{5CQA}^{\cdot} + R^- \quad (8)$$

* Corresponding author.
E-mail address: jelena.tosovic@kg.ac.rs (J. Tošović).

http://dx.doi.org/10.1016/j.foodchem.2017.05.080
0308-8146/

$$\mathbf{5CQA} + R^- \rightarrow \mathbf{5CQA}^- + RH \quad (9)$$

$$\mathbf{5CQA} + R^{\cdot} \leftrightarrows \mathbf{5CQA}^{+\cdot} + R^- \quad (10)$$

$$\mathbf{5CQA}^{+\cdot} + R^- \rightarrow \mathbf{5CQA}^{\cdot} + RH \quad (11)$$

In Eqs. (5)–(11) **5CQA**$^{\cdot}$, (**5CQA-R**)$^{\cdot}$, **5CQA**$^-$, and **5CQA**$^{+\cdot}$ denote the radical, radical adduct, anion, and radical cation, respectively, of the parent polyphenol **5CQA**; whereas R$^{\cdot}$ and R$^-$ stand for the present free radical and corresponding anion.

5CQA (Fig. 1) is an ester of caffeic and quinic acids. It is an important secondary metabolite in plants that plays various roles. This compound is a potent antioxidant that protects plants from lipid peroxidation (Kasai, Fukada, Yamaizumi, Sugie, & Mori, 2000). It has been reported that enhanced levels of **5CQA** in transgenic tomato plants increase microbial resistance and improve protection from UV radiation (Niggeweg, Michael, & Martin, 2004). It has been put forward that **5CQA** contributes to pest resistance in ornamental plants (Leiss, Maltese, Choi, Verpoorte, & Klinkhamer, 2009).

5CQA has been isolated at considerable amounts from coffee, potatoes, tomatoes, and eggplants, as well as from plums, apples, pears, and blueberries (Wang, Wang, & Yang, 2007). The green coffee extract is an ingredient of some encapsulated food supplements, conventional coffee products, and beverages (Farah, Monteiro, Donangelo, & Lafay, 2008). Like other dietary polyphenols, **5CQA** exhibits various biological and pharmacological effects, such as antihypertensive, antimutagenic, antitumor, anti-obesity, antidiabetic, hypolipidemic, anti-inflammatory, and antioxidative (Ong, Hsu, & Tan, 2013; Suzuki et al., 2006; Xu, Hu, & Liu, 2012).

A comparative theoretical study of the antioxidative activities of the caffeoylquinic (chlorogenic, neochlorogenic, and cryptochlorogenic) and caffeic acids has been recently performed by focusing on the thermodynamics of the HAT, SPLET, and SET-PT mechanisms (Marković & Tošović, 2016b; Chen, Xiao, Zheng, & Liang, 2015; Uranga, Podio, Wunderlin, & Santiago, 2016). It has been revealed that all four acids are characterized with very similar values of the corresponding reaction enthalpies, thus indicating that antioxidative activity of these acids does not depend on the esterification position. This finding is in perfect accord with the results of different experimental assays (Xu et al., 2012). It has been suggested that HAT may be the predominant mechanism in nonpolar solvents, while HAT and SPLET are competitive pathways in polar media (Marković & Tošović, 2016b, Chen et al., 2015). Bearing in mind that **5CQA** contains a conjugated chain attached to the aromatic ring, one can suppose that this compound can undergo RAF antioxidative pathway with small free radicals (Leopoldini, Chiodo, Russo, & Toscano, 2011).

However, the mechanisms of antioxidative action of this important ingredient of various foods and beverages have not been fully clarified. The present paper is an extension of our efforts devoted to the elucidation of antioxidative activity of **5CQA**. Electron spin resonance (ESR) spectroscopy and density functional theory (DFT) were utilized to examine the reactivity of **5CQA** towards selected radical species, with an emphasis on the mechanistic insight into the HAT, RAF, SPLET, and SET-PT reaction pathways.

2. Materials and methods

2.1. Chemicals

5CQA, DPPH$^{\cdot}$ (2,2-diphenyl-1-picrylhydrazyl), H_2O_2, $FeSO_4$, and DTPA (diethylenetriaminepentaacetic acid) were purchased from Sigma Aldrich, Taufkirchen, Germany. DEPMPO spin-trap (5-(diethoxyphosphoryl)-5-methyl-1-pyrroline-*N*-oxide) was provided by Enzo Life Sciences Inc., Farmingdale, NY, USA. DEPMPO spin-trap was purified and tested for hydroxylamine impurities using an established procedure (Jackson, Liu, Liu, & Timmins, 2002). Deionized 18 MΩ H_2O was used in the experiments.

2.2. ESR measurement

The ESR spectra were recorded at room temperature using a Bruker Elexsys E540 ESR spectrometer (Bruker, Billerica, MA,

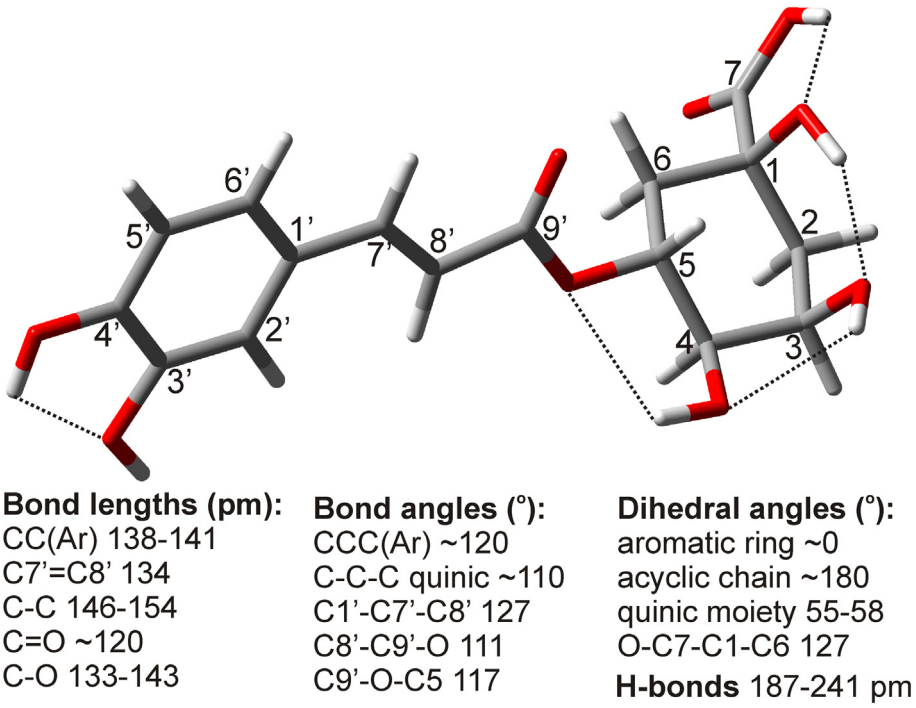

Fig. 1. Optimized structure of the preferential solvated conformer of chlorogenic acid (Marković, Tošović, & Dimitrić Marković, 2016a) with the key geometrical features. The atom labelling scheme is the same throughout the text.

USA) operating at X-band (9.51 GHz) with the following settings: modulation amplitude – 1 G; modulation frequency – 100 kHz; microwave power – 10 mW. The spectra were recorded using the EXepr software (Bruker BioSpin). The samples of **5CQA** were drawn into 10 cm long gas-permeable Teflon tubes (Zeus industries, Raritan, USA) (wall thickness 0.025 mm and internal diameter 0.6 mm). All measurements were performed under normal conditions, using quartz capillaries into which Teflon tubes were placed.

The DPPH· experiments were performed using 1 mM ethanol solution of DPPH· as control. The samples were incubated for 20 min at room temperature, and the measurements were conducted with 4 min scanning time. The relative ESR peak height of the middle peak in the ESR signal was measured.

The ability of **5CQA** to scavenge the HO· radicals was tested using the Fenton reaction as an "HO· producing" system, and DEPMPO spin-trap as control. The Fenton reaction system contained 5 mM H_2O_2, 5 mM $FeSO_4$, and 100 mM spin-trap. The pH value of the system was 3.5.

The ability of **5CQA** to remove the $O_2^{\cdot-}$ radicals was investigated using riboflavine-light system as the superoxide radical generator. The oxygen enriched riboflavine 0.05 mM solution, in the presence of DTPA and 100 mM DEPMPO spin-trap, was UV irradiated for 2 min and used as control. The pH value of the system was 3.9.

The amplitude of the third low-field ESR peak was measured in the case of both oxygen-centred radicals. This ESR signal originated from the corresponding spin-adduct formed during a 5-min period.

The above described control systems were compared to the corresponding systems where 1 mM **5CQA** was added. The capacity of **5CQA** to eliminate free radicals was evaluated based on the difference between the relative amplitudes of the ESR signals obtained with and without the addition of **5CQA**. The antioxidative activity (*AA*) was calculated as the relative decrease in radical production:

$$AA = 100 \times (I_0 - I_a)/I_0 \quad (12)$$

In Eq. (12) I_0 stands for the relative height of the corresponding ESR peak in the spectrum of the control system, and I_a denotes the relative height of the same ESR peak in the spectrum of the sample containing **5CQA**.

2.3. Computational methodology

2.3.1. General details

The M06-2X functional (Zhao & Truhlar, 2008) in combination with the 6-311++G(d,p) basis set and CPCM polarizable continuum solvation model (Cossi, Rega, Scalmani, & Barone, 2003), as implemented in Gaussian 09 software package (Frisch et al., 2010), was used for all calculations within this work. The exact same theoretical model has recently demonstrated robustness and very good overall performance in investigations of the related problems (Marković & Tošović, 2016b).

Geometrical parameters of all participants in investigated reactions were obtained by full optimizations, including frequency calculations, in benzene (dielectric constant $\varepsilon = 2.2706$), ethanol ($\varepsilon = 24.8520$), and water ($\varepsilon = 78.3553$). The restricted and unrestricted calculation schemes were applied for the closed-shell and open-shell structures. It was found, in the case of the radical species, that the eigenvalues of the total spin-squared operator $\hat{S}^2$ are very close to 0.75, which is the expected value for doublet spin states. This finding indicates insignificant spin contamination of the corresponding wave functions. The nature of the revealed stationary points on potential energy surface was confirmed by analyzing the results of the frequency calculations: no imaginary frequencies for equilibrium geometries, and exactly one imaginary frequency for transition states. The transition state structures were additionally examined by performing the IRC (intrinsic reaction coordinate) calculations. These calculations proved that each transition state (TS) connects two corresponding energy minima: reactant complex (RC) and product complex (PC). The natural bond orbital (NBO) analysis (Weinhold & Landis, 2012) was performed for hydrated **5CQA** molecule to gain the partial charges and Wiberg bond orders (Wiberg, 1968). To inspect the reliability of the CPCM solvation model, a selected pathway was investigated by adding three discrete water molecules into the reaction system. The role of these water molecules was to mimic hydrogen bond interactions, while the effects of bulk water were assessed by means of the CPCM solvation model.

2.3.2. Calculation of reaction energies and rate constants

In the thermodynamic approach, the reactions (5)–(11) were considered as the reactions of **5CQA** with four radical species: $O_2^{\cdot-}$, HOO·, HO·, and DPPH·. The free energies and enthalpies of the reactions at T = 298.15 K in the three solvents were determined. The free energy and enthalpy values of the solvated proton [Eq. (7)] in benzene (−901.8 and −898.7 kJ mol^{-1}), ethanol (−1065.5 and −1065.1 kJ mol^{-1}), and water (−1056.7 and −1052.7 kJ mol^{-1}) were taken from literature (Fifen et al., 2011; Marković, Tošović, Milenković, & Marković, 2016).

The kinetic approach was realized by simulating the reactions of **5CQA** with hydroxyl radical. This task was divided into two parts: the one where TS exists between the reactants and products [HAT and RAF, Eqs. (5) and (6)], and the other where there is no TS between the reactants and products [SPLET and SET-PT, Eqs. (7)–(11)]. All examined reactions are bimolecular (Fernàndez-Ramos, Miller, Klippenstein, & Truhlar, 2006). In all cases, the starting point was the Eyring equation and 1 M standard state. This equation, often called transition state theory (TST), turned out to be the most convenient way to interpret the thermal rate constants in contemporary solution phase kinetics:

$$k_{TST} = \frac{k_B T}{h} \exp(-\Delta G_a^{\ddagger}/RT) \quad (13)$$

In Eq. (13) k_B and h stand for the Boltzman and Planck constants, and $\Delta G_a^{\ddagger}$ is the free energy of activation. In the case of HAT and RAF mechanisms, reaction path degeneracy (σ) and transmission coefficient $\gamma(T)$ were taken into account, implying that the Eyring equation was transformed into:

$$k_{ZCT-0} = \sigma\gamma(T)\frac{k_B T}{h} \exp(-\Delta G_a^{\ddagger}/RT) \quad (14)$$

The reaction path degeneracy accounts for the number of equivalent reaction paths, i.e. it considers that a reaction can take place in different but equivalent ways. The transmission coefficient corrects for tunnelling effects (defined as the Boltzman average of the ratio between the quantum and classical probabilities), nonseparability of the reaction coordinate, and nonequilibrium reactants. The rate constants were determined by means of TheRate program (Duncan, Bell, & Truong, 1998). The k_{ZCT-0} values were calculated using the Eckart method (Eckart, 1930), also referred to as ZCT-0. The energy values and partition functions were taken from the quantum mechanical calculations.

In the case of the SPLET and SET-PT mechanisms the Marcus theory (Marcus, 1993) was used to estimate the activation barriers for the electron transfer (ET) reactions (8) and (10):

$$\Delta G_{aET}^{\ddagger} = \frac{\lambda}{4}\left(1 + \frac{\Delta_r G}{\lambda}\right)^2 \quad (15)$$

In Eq. (15) $\Delta_r G$ is the reaction free energy, whereas λ denotes the reorganization energy that was estimated as follows (Martínez, Hernández-Martin, & Galano, 2012; Nelsen et al., 2006):

$$\lambda \approx \Delta E - \Delta_r G \quad (16)$$

where ΔE is the non-adiabatic difference in total energy between the vertical products and reactants. Some rate constants obtained by inserting Eq. (15) into Eq. (13) were close to the diffusion limit. For this reason, the apparent rate constants (k_{app}) were obtained using the Collins-Kimball theory (Collins & Kimball, 1949):

$$k_{app} = \frac{k_D k_{TST}}{k_D + k_{TST}} \quad (17)$$

where k_D stands for the steady state Smoluchowski (Smoluchowski, 1917) rate constant for an irreversible bimolecular diffusion controlled reaction:

$$k_D = 4\pi\alpha D N_A \quad (18)$$

In Eq. (18) N_A denotes the Avogadro number, α stands for the reaction distance (calculated as the sum of the reactants radii: $\alpha = \alpha_{R1} + \alpha_{R2}$), and D is the mutual diffusion coefficient of the reactants (calculated as the sum of the reactants diffusion coefficients: $D = D_{R1} + D_{R2}$). Diffusion coefficients were calculated using the Stokes-Einstein approach:

$$D_{R1(R2)} = \frac{k_B T}{6\pi\eta\alpha_{R1(R2)}} \quad (19)$$

where η represents the solvent viscosity ($\eta = 0.6028 \times 10^{-3}$, 1.078×10^{-3}, and 0.8905×10^{-3} Pa·s for benzene, ethanol, and water, respectively).

3. Results and discussion

3.1. Interpretation of ESR spectra

ESR spectroscopy was utilized to examine the reactivity of **5CQA** towards DPPH$^{\cdot}$, HO$^{\cdot}$, and $O_2^{\cdot-}$ radical species. DPPH$^{\cdot}$ was chosen because it is the basis of commonly used antioxidant assays, whereas $O_2^{\cdot-}$ and HO$^{\cdot}$ were selected for their biological significance.

Taking into account that the ESR experiments were performed in acidic environment, the equilibrium in Eq. (1) is shifted to the right, implying that the superoxide radical anion existed as a mixture HOO$^{\cdot}$/$O_2^{\cdot-}$. According to the ESR measurements **5CQA** was selective towards DPPH$^{\cdot}$, HO$^{\cdot}$, and HOO$^{\cdot}$/$O_2^{\cdot-}$ (Fig. 2). It was observed that **5CQA** quenched ESR signals to different extents, suggesting different radical scavenging activities. The calculated reduction was 95.1% for DPPH$^{\cdot}$, 68.4% for HO$^{\cdot}$, and 34.4% for HOO$^{\cdot}$/$O_2^{\cdot-}$, indicating the highest activity of **5CQA** towards the DPPH$^{\cdot}$ radical. The lowest reactivity of HOO$^{\cdot}$/$O_2^{\cdot-}$ is expected. The reactivity of the other two radicals towards **5CQA** is in accord with the results of similar investigations related to **5CQA** containing extracts (Stanojević et al., 2009) and other polyphenolic compounds (Dimitrić Marković et al., 2012), where DPPH$^{\cdot}$ exhibited higher reactivity than HO$^{\cdot}$.

3.2. DFT study: thermodynamic and kinetic investigations

3.2.1. Thermodynamic approach

To provide additional insight into the reactivity of the utilized radicals towards **5CQA** the free energies and enthalpies of the reactions (5)–(11) in benzene, ethanol, and water were examined. Note that a preferential conformation of **5CQA** in solution (Fig. 1) has recently been deduced from the sophisticated NMR experiments (Forino et al., 2015) and comprehensive conformational analysis combined with different spectroscopic measurements (Marković et al., 2016a). This conformer was used in the thermodynamic approach to construct the free radicals, radical adducts, anions, and radical cation of **5CQA**. The free radicals (**5CQA3′**$^{\cdot}$ and **5CQA4′**$^{\cdot}$), anions (**5CQA3′**$^{-}$ and **5CQA4′**$^{-}$), and radical cation (**5CQA**$^{+\cdot}$) of **5CQA** have recently been examined in detail (Marković & Tošović, 2016b). Here, the properties of the products of radical adduct formation between **5CQA** and $O_2^{\cdot-}$, HOO$^{\cdot}$, and HO$^{\cdot}$ will be presented. Since both DPPH$^{\cdot}$ and **5CQA** are voluminous molecules, a pronounced steric hindrance can be expected in the process of binding of DPPH$^{\cdot}$ to **5CQA**. For this reason, the (**5CQA-DPPH**)$^{\cdot}$ radical adducts were not considered in this study.

There are nine suitable positions in **5CQA** where small free radicals can bind. The structures of all the (**5CQA-O$_2$**)$^{-\cdot}$, (**5CQA-HOO**)$^{\cdot}$, and (**5CQA-HO**)$^{\cdot}$ adducts in benzene, ethanol, and water solution, as well as the corresponding reaction energies were determined. The geometries of the radical adducts in water are presented in Figs. S1–S3, whereas the reaction free energies and enthalpies are collected in Table S1. Addition of $O_2^{\cdot-}$ to **5CQA** in positions 2′ and 3′ yields the products of addition of HOO$^{\cdot}$ to **5CQA**$^{-}$, as the radical anion takes a proton from the adjacent phenolic group (Fig. S1).

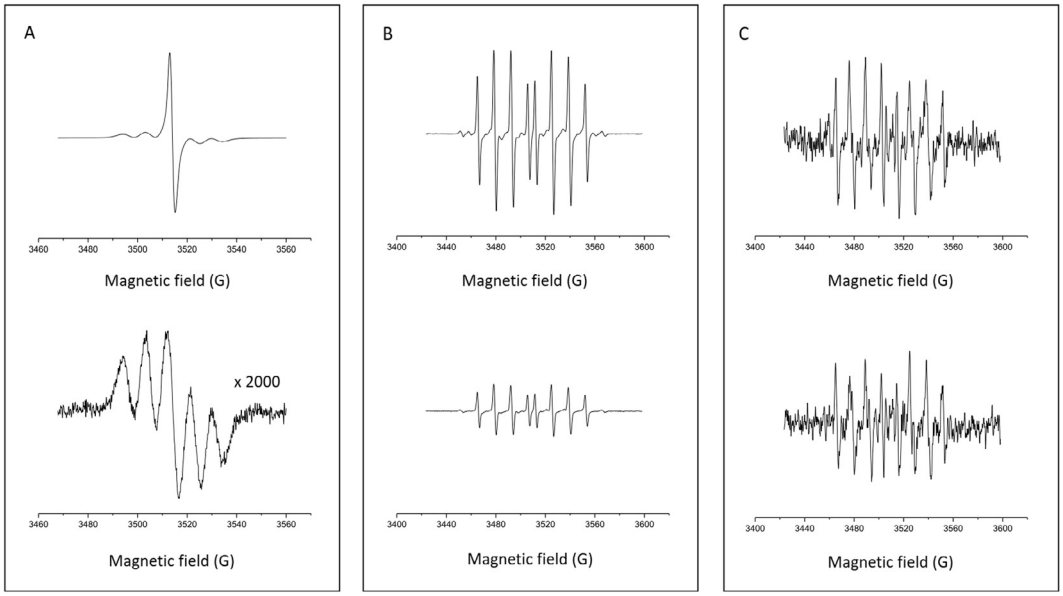

Fig. 2. ESR spectra of control samples (up) and samples in the presence of 1 mM chlorogenic acid (down): (A) DPPH$^{\cdot}$, (B) DEPMPO/HO$^{\cdot}$ adduct, (C) DEPMPO/HOO$^{\cdot}$ adduct. All comparable ESR spectra are given using the same relative intensity scale, except for (A).

Table 1
Reaction free energies (kJ mol^{-1}) related to Eqs. (5)–(11).

Position in **5CQA**[*]	Radical	HAT	RAF	SPLET			SET-PT	
		Eq. (5)	Eq. (6)	Step 1 Eq. (7)	Step 2 Eq. (8)	Step 3 Eq. (9)	Step 1 Eq. (10)	Step 2 Eq. (11)
		Benzene						
3′/7′	$O_2^{-\cdot}$	73.5	7.6		586.9	-40.6	887.6	-814.0
4′/9′		63.8	-22.6		596.1	-59.5		-823.8
3′/7′	HOO·	-18.6	26.1		114.1	-132.7	414.8	-433.4
4′/8′		-28.4	11.4	3′/4′ 363.5/344.5	123.3	-151.6		-443.1
3′/7′	HO·	-150.7	-81.8		38.8	-189.5	339.4	-490.1
4′/8′		-160.5	-101.8		47.9	-208.4		-499.9
3′	DPPH·	13.3	/		-33.8	47.1	266.8	-253.6
4′		3.5	/		-24.7	28.2		-263.3
		Ethanol						
3′/7′	$O_2^{-\cdot}$	64.2	59.1		302.8	5.7	458.1	-539.5
4′/9′		55.1	30.5		306.7	-7.4		-548.6
3′/7′	HOO·	-19.0	27.0		58.5	-77.5	213.8	-232.8
4′/8′		-28.0	15.7	3′/4′ 131.2/118.1	62.5	-90.5		-241.9
3′/7′	HO·	-152.8	-79.6		-28.3	-124.5	127.0	-279.8
4′/8′		-161.9	-99.7		-24.4	-137.5		-288.9
3′	DPPH·	15.4	/		-16.8	32.2	138.5	-123.1
4′		6.3	/		-12.8	19.1		-132.2
		Water						
3′/7′	$O_2^{-\cdot}$	63.5	62.4		283.5	8.5	428.3	-364.8
4′/9′		54.4	33.3		287.0	-4.0		-373.9
3′/7′	HOO·	-19.0	27.1		54.9	-73.9	199.8	-218.8
4′/8′		-28.1	16.1	3′/4′ 135.0/122.4	58.4	-86.5		-227.9
3′/7′	HO·	-152.9	-79.5		-32.7	-120.3	112.2	-265.1
4′/8′		-162.0	-100.3		-29.2	-132.8		-274.2
3′	DPPH·	15.5	/		-15.4	30.9	129.4	-114.0
4′		6.4	/		-11.9	18.3		-123.0

[*] Positions 3′ and 4′ refer to the HAT, SPLET, and SET-PT mechanisms, whereas 7′, 8′, and 9′ refer to the RAF mechanism.

Table S1 shows that $\Delta_r G$ values are significantly larger than the corresponding $\Delta_r H$ values. This occurrence is a consequence of the fact that RAF involves two reactants and one product, which causes negative entropy change because of a higher degree of order. As expected, positions 1′–6′ are not preferred for addition of radicals, as such addition leads to the aromaticity disturbance. Addition to the C7′ = C8′ double bond is thermodynamically less unfavourable. Partially negatively charged C8′ is particularly attractive for electrophilic HO· and HOO· (Fig. S4). Being characterized with noticeable partial positive charge, carbonyl C9′ is the most unfavourable position for attack of such free radicals, but the most attractive site for negatively charged $O_2^{-\cdot}$.

The reaction free energies and enthalpies related to the examined four mechanisms in benzene, ethanol, and water are summarized in Tables 1 and S2. The results for only two most favoured positions for the RAF mechanism (9′ and 7′) are presented. A general impression is that, unlike other radicals, $O_2^{-\cdot}$ is more reactive in benzene, whereas in the polar solvents the radical anion is solvated, and its reactivity suppressed. Both tables show that HAT and RAF only slightly depend on the solvent polarity. An exception is RAF with $O_2^{-\cdot}$ which is less favourable in polar solvents. Other two radicals are expected to bind to **5CQA**, where the formation of (**5CQA-HO**)· is both exergonic and exothermic. According to the reaction energies, HAT is thermodynamically favourable for all radicals except for $O_2^{-\cdot}$. Slightly positive $\Delta_r G$ and $\Delta_r H$ values in Eq. (5) with DPPH· are caused by better delocalization of the unpaired electron in DPPH· (larger molecule with three aromatic rings) than in **5CQA**·.

Step 1 of the SPLET mechanism is endergonic and endothermic, indicating that even in the polar solvents heterolytic cleavage of the O—H bonds is not plausible, and SPLET should not be considered in neutral and acidic media. There are six acidic hydrogens in **5CQA** molecule (Fig. S4) whose NBO charges in water solution are as follows: 0.50 (H3 and H4), 0.51 (H3′ and H4′), and 0.52 (H1 and H7). In agreement with the NBO charges are the Wiberg bond orders whose values are proportional to the O—H bond strengths. Namely, these values are equal to 0.69 for the O1–H1 and O7–H7 bonds, whereas the bond orders for other O—H bonds lie in the range of 0.73–0.74. One can suppose that the presence of a base will facilitate the formation of different anions of **5CQA**. However, the reactivity of the hydroxyl groups cannot be reliably predicted based on slight differences in partial charges and bond orders. On the other side, standard analytical approach (Galano & Alvarez-Idaboy, 2013) that uses experimental pK_a values of **5CQA** (3.35, 8.21, and 12.5 (Kiss et al., 1989)) shows that aqueous solution of **5CQA** contains 87% of monoanions and 13% of dianions at physiological pH of 7.4. It is reasonable to expect that dianions have a strong tendency to undergo ET reactions. However, this very interesting and complex problem is beyond the scope of this work. Namely, to extend our recent work where SPLET of **5CQA** was considered through the proton affinity and electron transfer enthalpy (Marković & Tošović, 2016b), we are here focused on the role of the phenolate anions **5CQA3′**$^-$ and **5CQA4′**$^-$. Our preliminary investigations showed that in basic environment **5CQA** forms three monoanions: carboxylate anion and two phenolate anions. Carboxylate anion is the most abundant, but it is not able to spontaneously donate an electron to any of the examined radicals. Phenolate anions are present at very low concentrations (around 0.03%), but they can participate in step 2 to yield R$^-$, which can further act as a base in step 3. Different reactive species behave differently in Eqs. (8) and (9). $O_2^{-\cdot}$ can act as a base with **5CQA** to build **5CQA**$^-$ and HOO· [Eq. (9)], implying that step 1 can be avoided in this case. Tables 1 and S2 show that this reaction is energetically favoured, particularly in benzene, but one needs to bear in mind that the existence of $O_2^{-\cdot}$ is also conditioned by larger pH values. The so-formed **5CQA**$^-$ can participate in Eq. (8) with either $O_2^{-\cdot}$ (extremely unfavourable) or HOO· (less unfavourable). In general, step 2 of the SPLET mechanism is facilitated in the polar solvents

where the charged species are stabilized. Finally, the reaction energies of step 3 indicate plausible action of the examined R^- anions as bases. Slightly positive $\Delta_r G$ and $\Delta_r H$ values in Eq. (9) with $DPPH^-$ are caused by better delocalization of the negative charge in $DPPH^-$ than in **5CQA**$^-$.

As for the SET-PT mechanism, step 2 is characterized with notably large negative reaction energies. However, step 1 is energetically extremely demanding, where $\Delta_r G$ and $\Delta_r H$ values decrease with the increasing solvent polarity.

Taking into account the experimental conditions of the ESR measurements and results of the thermodynamic consideration one can exclude a possibility that any of the examined free radicals undergoes the SPLET and SET-PT mechanisms. A finding that no mechanism is suitable for **5CQA** and $O_2^{\cdot-}$ in water solution confirms that HOO· is responsible for the behaviour of the HOO·/$O_2^{\cdot-}$ mixture in acidic environment. One may suppose that HAT and RAF are plausible reaction pathways of **5CQA** with the HOO· and HO· radicals. Despite very slight endergonicity, which can be attributed to better delocalization of the unpaired electron in DPPH· than in **5CQA**·, HAT is the only likely mechanism in the case of the DPPH· radical. It is well-known that some thermodynamically unfavourable reactions (whose reaction energies do not exceed 40–45 kJ mol^{-1}) pass through low-lying transition states, indicating that in such cases reaction kinetics can be the determining factor (Galano & Alvarez-Idaboy, 2013).

A careful inspection of Tables 1 and S2 reveals that majority of the reactions with HO· are characterized with negative $\Delta_r G$ and $\Delta_r H$ values, including RAF in all solvents, and both step 2 and step 3 of SPLET in the polar solvents. In addition, the energies of Eq. (10) with HO· in ethanol and water hardly exceed 120 and 110 kJ mol^{-1}, implying that even SET-PT deserves additional examination. Taking all these facts into account, HO· was selected for further kinetic investigations of all four antioxidative mechanisms.

3.2.2. Mechanistic approach

As we mentioned earlier, HAT and RAF are the mechanisms where transition states exist between the reactants and products. Optimized geometries for both transition states for the HAT, and nine transition states for the RAF mechanisms in water solution are depicted in Fig. 3. The results of the IRC calculations for two TSs are presented in Figs. S5 and S6.

The participants in the reaction of hydroxyl radical with **5CQA** involved in HAT mechanism in positions 3′ and 4′ in water solution are presented in Figs. S7 and S8. The reaction paths for these two positions are very similar. Both RCs are characterized with the existence of hydrogen bonds (187.6 pm and 186.7 pm for the positions 3′ and 4′) between HO· and the corresponding phenolic group. The reactions pass through TSs where simultaneous O—H bond cleavage of the phenolic group occurs, along with the formation of water molecule, and with the C3′—O3′ (C4′—O4′) bond shortening (Figs. 3, S7, and S8). In the PCs, the water molecule is hydrogen-bonded to the formed **5CQA**· radical, where PC3′ is characterized with one (186.9 pm), and PC4′ with two H—bonds (205.6 and 170.7 pm).

In the case of RAF mechanism, the reaction also starts with the formation of RCs. It should be noted that despite numerous attempts, we failed to locate some RCs. In the ethanol and water solutions the RCs in positions 3′, 5′, 7′, and 9′, whereas in benzene solution the RCs in positions 2′, 3′, and 7′ were not located. However, Fig. S9 (water solution) reveals that spin density is delocalized over C3′, C4′, and C5′ atoms in RC4′, whereas in RC8′ spin density is delocalized over C7′, C8′, and C9′ atoms. This finding indicates that the radical oxygen in each of these two RCs is capable of binding to all three corresponding carbons. There is an analogous situation with the RCs in benzene.

Fig. 3 reveals that majority of TSs involved in the RAF mechanism, except for TS1′ and TS9′, are early transition states. Two

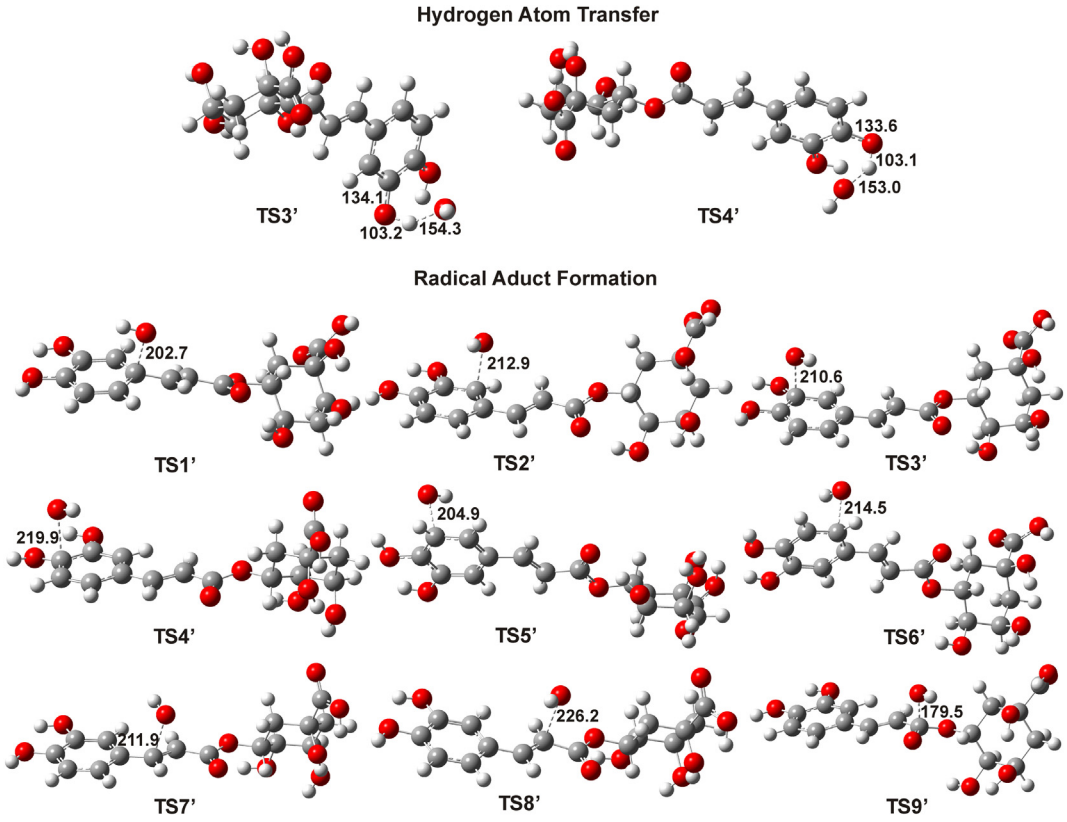

Fig. 3. Optimized geometries of TSs in positions 3′ and 4′ for HAT, and in positions 1′–9′ for RAF in water solution. The characteristic bond distances are given in pm.

Table 2
Gibbs energies of activation $\Delta G_a^{\ddagger}$ (kJ mol^{-1}) and rate constants (M^{-1} s^{-1}) for the reactions of **5CQA** with hydroxyl radical via HAT and RAF mechanisms. k_{TST} and $k_{ZCT\text{-}0}$ denote the rate constants calculated using TST and Eckart methods.

		Benzene			Ethanol			Water		
		$\Delta G_a^{\ddagger}$	k_{TST}	$k_{ZCT\text{-}0}$	$\Delta G_a^{\ddagger}$	k_{TST}	$k_{ZCT\text{-}0}$	$\Delta G_a^{\ddagger}$	k_{TST}	$k_{ZCT\text{-}0}$
HAT	3′	41.5	8.07×10^6	1.61×10^7	44.3	2.58×10^6	6.32×10^6	44.9	2.07×10^6	4.89×10^6
	4′	45.5	1.64×10^6	4.54×10^6	47.7	6.70×10^5	1.94×10^6	47.7	6.64×10^5	1.91×10^6
RAF	1′	52.7	8.84×10^4	1.21×10^5	52.6	9.38×10^4	1.21×10^5	51.0	1.76×10^5	2.25×10^5
	2′	36.8	5.35×10^7	2.89×10^7	35.1	1.07×10^8	9.19×10^7	34.8	1.21×10^8	1.04×10^8
	3′	40.3	1.30×10^7	1.55×10^7	39.7	1.72×10^7	2.02×10^7	39.7	1.65×10^7	1.94×10^7
	4′	26.5	3.43×10^9	8.44×10^7	29.5	1.04×10^9	1.59×10^8	29.6	9.94×10^8	1.77×10^8
	5′	36.9	5.18×10^7	3.73×10^7	43.2	4.14×10^6	5.22×10^6	44.4	2.49×10^6	3.12×10^6
	6′	36.6	5.77×10^7	6.82×10^7	33.3	2.53×10^8	2.74×10^8	33.0	2.48×10^8	2.63×10^8
	7′	39.9	1.56×10^7	1.94×10^7	37.4	4.42×10^7	4.95×10^7	37.1	4.83×10^7	5.55×10^7
	8′	25.4	5.50×10^9	5.82×10^7	20.0	4.82×10^{10}	3.38×10^8	20.0	4.86×10^{10}	3.31×10^8
	9′	101.6	2.36×10^{-4}	4.13×10^{-4}	104.5	7.50×10^{-5}	1.31×10^{-4}	104.6	7.00×10^{-5}	1.22×10^{-4}

examples of the reaction in water solution (positions 1′ and 8′) are shown in Figs. S10 and S11. RC1′ and RC8′ are characterized with relatively strong interactions of hydroxyl radical with π electrons of the aromatic ring and double bond. In the TSs significant C–O bond shortening occurs. Finally, the products are characterized with completely formed σ C–O bond (bond lengths are 144.4 and 143.4 pm for the positions 1′ and 8′). It is apparent from Fig. S10 that, as the reaction in position 1′ progresses, the reaction system becomes non-planar, and therefore, conjugation between the acyclic chain and aromatic ring is lost. The C6′—C1′—C7′—C8′ dihedral angle was found to be about 0°, 30° and 80° in the RC1′, TS1′ and corresponding product, respectively. In contrast, the same dihedral angle for all three participants in the reaction in position 8′ amounts to ∼0° (Fig. S11).

The activation Gibbs energies and rate constants at 298 K for all HAT and RAF reaction pathways in all three solvents were calculated and collected in Table 2. As expected, Gibbs activation energies and rate constants for both mechanisms are very slightly dependent on the solvent polarity. The activation energies for HAT mechanism in position 3′ are slightly lower and k_{TST} values are larger in comparison to those in position 4′, implying that reaction in position 3′ is slightly faster. However, reaction in position 4′ yields thermodynamically more stable radical product (Table 1). One can conclude that the HAT reaction paths in positions 3′ and 4′ are competitive.

The early TSs in RAF mechanism are reflected through small activation energies. The lowest Gibbs activation energies, as well as the largest k_{TST} values, indicate that reactions in positions 4′ and 8′ are the fastest. The small activation energy value for the reaction in position 4′ can be explained by stabilization of TS4′ caused by a hydrogen bond between the hydroxyl moiety and the proximate phenolic group (Fig. 3). However, this reaction pathway is thermodynamically less favourable (Table S1), due to disturbance of aromaticity in the benzene ring. From the kinetic point of view, 9′ and 1′ are the most unfavourable positions for addition of HO· because of already mentioned electrophilicity of C9′, and disruption of electron delocalization between the acyclic chain and aromatic ring.

A comparison of k_{TST} and $k_{ZCT\text{-}0}$ values shows that, at temperature of 298 K, the two rate constants for both positions in HAT in all three solutions practically coincide (Table 2), indicating that both TST (Eq. (13)) and Eckart (Eq. (14))) methods are suitable for assessing the rates of these reactions at room temperature. The differences between the rate constant values are noticeable at lower temperatures (Fig. S12). Taking into account that HAT mechanism involves light hydrogen atoms capable of penetrating through activation barriers, these differences between the k_{TST} and $k_{ZCT\text{-}0}$ values can be attributed to the tunnelling effect. The tunnelling effect rapidly decreases with the increasing temperature, which is to some extent a consequence of the well-known fact that Eckart method overestimates this effect at low temperatures. Fig. S13 shows that almost all RAF pathways (except for 4′ and 8′) show consistency between the k_{TST} and $k_{ZCT\text{-}0}$ values, indicating that the $\gamma(T)$ values are close to unity at all temperatures. In positions 4′ and 8′ k_{TST} decreases with increasing temperature, and $k_{ZCT\text{-}0}$ values are significantly smaller at all temperatures. It is apparent that the conventional TST is not adequate for evaluating the rates of the 4′ and 8′ RAF pathways. Bearing in mind that these two paths are characterized with the smallest activation energy values, the failure of TST can be ascribed to the flat potential energy surfaces.

It is well-known that hydrogen bonds, particularly in polar solvents, can influence both kinetics and thermodynamics of the reactions of HO·. For this reason, the 8′ RAF pathway was investigated by adding three discrete water molecules in the vicinity of the reaction centre (Fig. S14). The obtained results are very similar to those presented in Tables 1 and 2. Namely, the values of $\Delta_r G$ and $\Delta G_a^{\ddagger}$ amount to −105.1 and 23.6 kJ mol^{-1}, and the corresponding rate constants k_{TST} and $k_{ZCT\text{-}0}$ are 1.14×10^{10} and 0.78×10^8 M^{-1} s^{-1}. This consistency between the two sets of results indicates high reliability of the CPCM solvation model.

When the SPLET mechanism was considered it was assumed that it occurs in basic environment, implying that step 1 can be presented as: **5CQA** + B$^-$ → **5CQA3′**$^-$ (**5CQA4′**$^-$) + BH, where B$^-$ represents the base. In all three solvents, step 1 was simulated by employing HO$^-$, HOO$^-$, O_2^{2-}, and methylamine as the bases that attacked H3′ and H4′. No transition states were located. Furthermore, our numerous attempts to optimize reactant complexes yielded product complexes: **5CQA3′**$^-$ or **5CQA4′**$^-$ and corresponding protonated base, followed with release of energy. These facts indicate that formation of anionic initiators proceeds spontaneously in the presence of either strong or weak bases, thus enabling the next step of chain reaction, electron transfer (ET), to occur. Following the above described procedure, the activation barriers and rate constants for ET were determined. The results for all three solvents are presented in Table 3.

It is apparent from Table 3 that solvent polarity significantly affects electron transfer reactions. Namely, the activation energies and corresponding rate constants reveal that electron transfer in nonpolar benzene is much slower than in polar ethanol and water. The values of k_{TST} and k_{app} are practically identical in benzene solution indicating that the rates of electron transfer are far from the rates of diffusion controlled reactions. On the other hand, the values of k_{TST} in ethanol and water are extremely high, so that further calculations lead to drastically reduced values for k_{app}. Taking into account that values for k_D and k_{app} are mutually very similar in

Table 3
Results related to electron transfer from positions 3′ and 4′ of **5CQA**$^-$ to HO$^\cdot$ in the three solvents.*

Solvent	Position	$\Delta G^{\ddagger}_{aET}$ kJ mol^{-1}	λ kJ mol^{-1}	k_{TST} M^{-1} s^{-1}	k_D M^{-1} s^{-1}	k_{app} M^{-1} s^{-1}
Benzene	3′	42.2	21.5	2.46×10^5	1.27×10^{10}	2.46×10^5
	4′	58.5	19.3	3.52×10^2	1.28×10^{10}	3.52×10^2
Ethanol	3′	1.3	18.5	3.68×10^{12}	7.14×10^9	7.13×10^9
	4′	1.4	15.2	3.54×10^{12}	7.15×10^9	7.14×10^9
Water	3′	2.8	18.3	1.99×10^{12}	8.44×10^9	8.40×10^9
	4′	3.3	15.0	1.60×10^{12}	8.40×10^9	8.35×10^9

* $\Delta G^{\ddagger}_{aET}$ and λ denote activation free energy and reorganization energy, whereas k_{TST}, k_D, and k_{app} stand for the rate constant arising from TST, rate constant for an irreversible bimolecular diffusion controlled reaction, and apparent rate constant, respectively.

polar solvents, one can conclude that in such environment ET from **5CQA**$^-$ to HO$^\cdot$ is a diffusion controlled reaction. Independently of solvent polarity, the k_{app} values are large enough to propagate the chain reaction by producing the hydroxide anions.

The free energy of activation for step 1 of the SET-PT mechanism, i.e. ET from **5CQA** to HO$^\cdot$ was estimated by employing Eq. (15). $\Delta G^{\ddagger}_{aET}$in benzene is so large that the corresponding rate constant practically equals zero. The $\Delta G^{\ddagger}_{aET}$ values in ethanol and water solutions amount to 262.4 and 213.3 kJ mol^{-1}, and the rate constants are equal to 6.53×10^{-34} and 2.63×10^{-25} M^{-1} s^{-1}, respectively. The obtained values demonstrate that the equilibrium in Eq. (10) is completely shifted to the left. In accord with this finding are our attempts to optimize HO$^-$ and **5CQA**$^{+\cdot}$ together, which all yielded different reactant complexes consisting of HO$^\cdot$ and **5CQA.** A reason for this occurrence can be the fact that the HOMO energy of HO$^-$ is higher than the SOMO energy of **5CQA**$^{+\cdot}$ in all solvents (for example the HOMO and SOMO energies in water solution are -0.26854 and -0.32179 au), and an electron spontaneously transfers from the anion to the radical cation. These facts indicate that reaction (11) cannot occur at all. In other words, SET-PT is not a plausible reaction path of **5CQA** even with highly reactive and electrophilic HO$^\cdot$.

4. Conclusions

According to the ESR measurements, **5CQA** was selective towards the DPPH$^\cdot$, HO$^\cdot$, and HOO$^\cdot$/$O_2^{-\cdot}$ radicals. Our results are in accord with literature data that claim that DPPH$^\cdot$ generally shows high reactivity towards all phenolic acids and their esters (Mathew, Abraham, & Zakaria, 2015).

Taking into account that the ESR measurements were performed in acidic media, the results of the thermodynamic examination exclude a possibility that any of the examined free radicals ($O_2^{-\cdot}$, HOO$^\cdot$, HO$^\cdot$, and DPPH$^\cdot$) undergoes the SPLET and SET-PT mechanisms. The finding that no mechanism is suitable for **5CQA** and $O_2^{-\cdot}$ in water solution confirms that HOO$^\cdot$ is responsible for the behaviour of the HOO$^\cdot$/$O_2^{-\cdot}$ mixture in acidic environment. One may suppose that HAT and RAF are plausible reaction pathways of **5CQA** with the HOO$^\cdot$ and HO$^\cdot$ radicals, whereas HAT is the only expected mechanism in the case of the DPPH$^\cdot$ radical.

Thermodynamic consideration agrees with mechanistic investigation of the four mechanisms of **5CQA** with HO$^\cdot$. SPLET and SET-PT are facilitated in polar solvents. However, SET-PT is not a plausible antioxidative pathway of **5CQA** in any medium because of the pronounced endergonicity (endothermicity) and extremely large free energy of activation for electron transfer from **5CQA** to HO$^\cdot$. SPLET should not be considered in neutral and acidic media because of energetically highly demanding heterolytic cleavage of the phenolic O—H bonds. In the presence of either strong or weak bases this cleavage proceeds spontaneously, and yields phenolate anions **5CQA**$^-$ at very low concentration. In this way, the next step, ET from **5CQA**$^-$ to HO$^\cdot$, is enabled to occur. In ethanol and water this ET is a diffusion controlled reaction. Independently of solvent polarity, the rate constants are large enough to propagate the chain reaction by producing the hydroxide anions. These findings indicate that at physiological pH of 7.4, SPLET is the likely antioxidative mechanism of **5CQA** with extremely high rate. Certainly, the influence of dianions on the SPLET mechanism of **5CQA** needs to be investigated.

The HAT and RAF mechanisms very slightly depend on solvent polarity. The two HAT pathways (3′ and 4′) are competitive, as they are kinetically and thermodynamically comparable. The tunnelling effect was observed at low temperatures. The RAF mechanism is generally characterized with early TSs, and accordingly, small activation energies, and large rate constants. Position 8′ is both kinetically and thermodynamically the most favourable site of **5CQA** for HO$^\cdot$ binding. When the rates of HAT and RAF are compared, the rate constants for RAF pathways are larger by at most two orders of magnitude. However, HAT yields thermodynamically more stable radical products. One can conclude that in acidic and neutral media **5CQA** and HO$^\cdot$ can take either HAT or RAF pathways.

The findings of this work confirm and complement the results of our related study (Marković & Tošović, 2016b). As it is well-known that caffeic and caffeoylquinic acids show very similar antioxidative activities (Marković & Tošović, 2016b; Kono et al., 1997; Xu et al., 2012) it is interesting to compare the results of the present work to those related to caffeic acid (Leopoldini et al., 2011). The two studies agree that RAF is faster than HAT. The rate constants obtained in the present work are by two or three orders of magnitude smaller than those of Leopoldini et al. (2011). These differences can be ascribed to the fact that the rates of Leopoldini et al. (2011) refer to the gas-phase, whereas the results of this study refer to three different solvents.

It is also intriguing to compare the results of computations to the experimental rates. It has been found, by means of pulse radiolysis, that the rate constant for the reaction of **5CQA** with HO$^\cdot$ amounts to $3.34 \pm 0.19 \times 10^9$ M^{-1} s^{-1} (Kono et al., 1997). This result agrees well with our results related to the SPLET mechanism. Taking into account that the experiment has been performed in basic environment (pH = 7.4), it is reasonable to assume that so large experimentally determined rate corresponds to electron transfer reaction.

Acknowledgement

This work was supported by the Ministry of Science and Technological Development of the Republic of Serbia (project nos. 172016, 172015 and 41005).

Appendix A. Supplementary data

Supplementary data associated with this article can be found, in the online version, at http://dx.doi.org/10.1016/j.foodchem.2017.05.080.

References

Chen, Y., Xiao, H., Zheng, J., & Liang, G. (2015). Structure-thermodynamics-antioxidant activity relationships of selected natural phenolic acids and derivatives: An experimental and theoretical evaluation. *PLoS ONE/ Public Library of Science, 10*, 1–20.

Collins, F. C., & Kimball, G. E. (1949). Diffusion-controlled reaction rates. *Journal of Colloid Science, 4*, 425–437.

Cossi, M., Rega, N., Scalmani, G., & Barone, V. (2003). Energies, structures, and electronic properties of molecules in solution with the C-PCM solvation model. *Journal of Computational Chemistry, 24*, 669–681.

Dimitrić Marković, J. M., Marković, Z., Pašti, I. A., Brdarić, T. P., Popović-Bijelić, A., & Mojović, M. (2012). A joint application of spectroscopic, electrochemical and theoretical approaches in evaluation of the radical scavenging activity of 3-OH flavones and their iron complexes towards different radical species. *Dalton Transactions, 41*, 7295–37303.

Duncan, W. T., Bell, R. L., & Truong, T. N. (1998). TheRate: Program for ab initio direct dynamics calculations of thermal and vibrational-state-selected rate constants. *Journal of Computational Chemistry, 19*, 1039–1052.

Eckart, C. (1930). The penetration of a potential barrier by electrons. *Physical Review, 35*, 1303–1309.

Farah, A., Monteiro, M., Donangelo, C. M., & Lafay, S. (2008). Chlorogenic acids from green coffee extract are highly bioavailable in humans. *The Journal of Nutrition, 138*, 2309–2315.

Fernàndez-Ramos, A., Miller, J. A., Klippenstein, S. J., & Truhlar, D. G. (2006). Modeling the kinetics of bimolecular reactions. *Chemical Reviews, 106*, 4518–4584.

Fifen, J. J., Nsangou, M., Dhaouadi, Z., Motopon, O., & Jaidane, N. (2011). Solvent effects on the antioxidant activity of 3,4-dihydroxyphenylpyruvic acid: DFT and TD-DFT studies. *Computational and Theoretical Chemistry, 966*, 232–243.

Forino, M., Tenore, G. C., Tartaglione, L., Dell'Aversano, C., Novellino, N., & Ciminiello, P. (2015). (1*S*,3*R*,4*S*,5*R*)5-O-Caffeoylquinic acid: Isolation, stereo-structure characterization and biological activity. *Food Chemistry, 178*, 306–310.

Frisch, M. J., Trucks, G. W., Schlegel, H. B., Scuseria, G. E., Robb, M. A., Cheeseman, J. R., et al. (2010). *Gaussian 09. Revision C.01*. Wallingford: Gaussian Inc.

Galano, A., Mazzone, G., Alvarez-Diduk, R., Marino, T., Alvarez-Idaboy, J. R., & Russo, N. (2016). The food antioxidants: chemical insights at the molecular level. *Annual Review of Food Science and Technology, 7*, 335–352.

Galano, A., & Alvarez-Idaboy, J. R. (2013). A computational methodology for accurate predictions of rate constants in solution: application to the assessment of primary antioxidant activity. *Journal of Computational Chemistry, 34*, 2430–2445.

Jackson, S. K., Liu, K., Liu, M., & Timmins, G. S. (2002). Detection and removal of contaminating hydroxylamines from the spin trap DEPMPO, and re-evaluation of its use to indicate nitrone radical cation formation and SN1 reactions. *Free Radical Biology and Medicine, 32*, 228–232.

Kasai, H., Fukada, Z., Yamaizumi, S., Sugie, S., & Mori, H. (2000). Action of chlorogenic acid in vegetables and fruits as an inhibitor of 8-hydroxydeoxyguanosine formation in vitro and in a rat carcinogenesis model. *Food and Chemical Toxicology, 38*, 467–471.

Kiss, T., Nagy, G., Pécsi, M., Kozlowski, H., Micera, G., & Erre, L. S. (1989). Complexes of 3,4-dihydroxyphenyl derivatives–X.* Copper(II) complexes of chlorogenic acid and related compounds. *Polyhedron, 8*, 2345–2349.

Kono, Y., Kobayashi, K., Tagawa, S., Adachi, K., Ueda, A., Sawa, Y., & Shibata, H. (1997). Antioxidant activity of polyphenolics in diets. Rate constants of reactions of chlorogenic acid and caffeic acid with reactive species of oxygen and nitrogen. *Biochimica et Biophysica Acta, 1335*, 335–342.

Leiss, K. A., Maltese, F., Choi, Y. H., Verpoorte, R., & Klinkhamer, P. G. (2009). Identification of chlorogenic acid as a resistance factor for thrips in Chrysanthemum. *Plant Physiology, 150*, 1567–1575.

Leopoldini, M., Chiodo, S. G., Russo, N., & Toscano, M. (2011a). Detailed investigation of the OH radical quenching by natural antioxidant caffeic acid studied by quantum mechanical models. *Journal of Chemical Theory and Computation, 7*, 4218–4233.

Leopoldini, M., Russo, N., & Toscano, M. (2011b). The molecular basis of working mechanism of natural polyphenolic antioxidants. *Food Chemistry, 125*, 288–306.

Litwinienko, G., & Ingold, K. U. (2007). Solvent effects on the rates and mechanisms of reaction of phenols with free radicals. *Accounts of Chemical Research, 40*, 222–230.

Marcus, R. A. (1993). Electron transfer reactions in chemistry. Theory and experiment. *Reviews of Modern Physics, 65*, 599–610.

Marković, S., Tošović, J., & Dimitrić Marković, J. M. (2016a). Synergic application of spectroscopic and theoretical methods to the chlorogenic acid structure elucidation. *Spectrochimica Acta. Part A: Molecular and Biomolecular Spectroscopy, 164*, 67–75.

Marković, S., & Tošović, J. (2016b). Comparative study of the antioxidative activities of caffeoylquinic and caffeic acids. *Food Chemistry, 210*, 585–592.

Marković, Z., Tošović, J., Milenković, D., & Marković, S. (2016). Revisiting the solvation enthalpies and free energies of the proton and electron in various solvents. *Computational and Theoretical Chemistry, 1077*, 11–17.

Martínez, A., Hernández-Martin, E., & Galano, A. (2012). Xanthones as antioxidants: A theoretical study on the thermodynamics and kinetics of the single electron transfer mechanism. *Food & Function, 3*, 442–450.

Mathew, S., Abraham, T. E., & Zakaria, Z. A. (2015). Reactivity of phenolic compounds towards free radicals under in vitro conditions. *Journal of Food Science and Technology, 9*, 5790–5798.

Mazzone, G., Malaj, N., Galano, A., Russo, N., & Toscano, M. (2015). Antioxidant properties of several coumarin–chalcone hybrids from theoretical insights. *RSC Advances, 5*, 565–575.

Nelsen, S. F., Weaver, M. N., Luo, Y., Pladziewicz, J. R., Ausman, L. K., Jentzsch, T. L., & O'Konek, J. J. (2006). Estimation of electronic coupling for intermolecular electron transfer from cross-reaction data. *The Journal of Physical Chemistry A, 110*, 11665–11676.

Niggeweg, R., Michael, A. J., & Martin, C. (2004). Engineering plants with increased levels of the antioxidant chlorogenic acid. *Nature Biotechnology, 22*, 746–754.

Ong, K.-W., Hsu, A., & Tan, B.-K. (2013). Anti-diabetic and anti-lipidemic effects of chlorogenic acid are mediated by ampk activation. *Biochemical Pharmacology, 85*, 1341–1351.

Smoluchowski, M. V. (1917). Versuch einer mathematischen Theorie der Koagulationskinetik kolloider Lösungen. *Zeitschrift fur Physikalische Chemie, 92*, 129–168.

Stanojević, Lj., Stanković, M., Nikolić, V., Nikolić, Lj., Ristić, D., Čanadanovic-Brunet, J., & Tumbas, V. (2009). Antioxidant activity and total phenolic and flavonoid contents of *Hieracium pilosella* L. extracts. *Sensors, 9*, 5702–5714.

Suzuki, A., Yamamoto, N., Jokura, H., Yamamoto, M., Fujii, A., Tokimitsu, I., & Saito, I. (2006). Chlorogenic acid attenuates hypertension and improves endothelial function in spontaneously hypertensive rats. *Journal of Hypertension, 24*, 1065–1073.

Uranga, J. G., Podio, N. S., Wunderlin, D. A., & Santiago, N. (2016). Theoretical and experimental study of the antioxidant behaviors of 5-O-caffeoylquinic, quinic and caffeic acids based on electronic and structural properties. *ChemistrySelect, 1*, 4113–4120.

Wang, X., Wang, J., & Yang, N. (2007). Chemiluminescent determination of chlorogenic acid in fruits. *Food Chemistry, 102*, 422–426.

Weinhold, F., & Landis, C. R. (2012). *Discovering chemistry with natural bond orbitals*. Hoboken: John Wiley & Sons Inc.

Wiberg, K. B. (1968). Application of the Pople-Santry-Segal CNDO method to the cyclopropylcarbinyl and cyclobutyl cation and to bicyclobutane. *Tetrahedron, 24*, 1083–1096.

Xu, J.-G., Hu, Q.-P., & Liu, Y. (2012). Antioxidant and DNA-protective activities of chlorogenic acid isomers. *Journal of Agricultural and Food Chemistry, 60*, 11625–11630.

Zhao, Y., & Truhlar, D. G. (2008). Density functionals with broad applicability in chemistry. *Accounts of Chemical Research, 41*, 157–167.